

Article

Arsenic-Induced Mitochondria-Mediated Apoptosis is Associated with PGC-1 α Decrease in Rat Brain

Bo Ding^{a†}, Xinbo Ma^{a†}, Yang Liu^{a†}, Bangyao Ni^a, Siqi Lu^a, Yuting Chen^a, Xiaona Liu^{a†*} and Wei Zhang^{a†*}

^aCenter for Endemic Disease Control, Chinese Center for Disease Control and Prevention, Harbin Medical University, Key Lab of Etiology and Epidemiology, Education Bureau of Heilongjiang Province & Ministry of Health (23618504), Harbin, 150081, China University, Harbin, 150001, China

† These authors contributed equally to the work and should be considered as first authors

‡ These authors contributed equally to the work and should be considered as corresponding authors

* Correspondence: xiaonaliu_2013@163.com or liuxiaona2017@hrbmu.edu.cn (Xiaona Liu); Telephone: 86 45187503105; zwhxd@126.com or zhangwei@hrbmu.edu.cn (Wei Zhang); Telephone: 86 45187503105

Abstract: Chronic exposure to arsenic in drinking-water damage to cognitive function, and nerve cells apoptosis is one of primary characteristic. The damage of mitochondrial structure and/or function is one of the main characteristics of apoptosis. Peroxisome proliferator activated receptor γ Coactivator α (PGC-1 α) is involved in the regulation of mitochondrial biogenesis, energy metabolism and apoptosis. In this study, we aimed to study role of PGC-1 α in sodium arsenite (NaAsO₂)-induced mitochondrial apoptosis in rat hippocampal cells. We discovered that arsenic-induced apoptosis increased in rat hippocampus increased with NaAsO₂ (0, 2, 10, and 50 mg/L, orally via drinking water for 12 weeks) exposure by TUNEL assay, and the structure of mitochondria was incomplete, swollen, lysosomes and lipofuscin increasing, and nuclear membrane shrunk observed by transmission electron microscope. Furthermore, NaAsO₂ reduced levels of Bcl-2 and PGC-1 α , increased the levels of Bax and Cytochrome C expression. Moreover, correlation analysis showed that brain arsenic content was negatively correlated with PGC-1 α level and brain ATP content, respectively; PGC-1 α level was negatively correlated with apoptosis rate; Brain ATP content was positively correlated with PGC-1 α level; but no significant correlation between ATP content and apoptosis has been observed in this study. Taken together, the results of present study indicate that NaAsO₂-induced mitochondrial pathway apoptosis is related to the reduction of PGC-1 α , accompanied by ATP depletion.

Keywords: Arsenic; PGC-1 α ; Mitochondria; Hippocampus; Apoptosis

1. Introduction

long-term drinking water contaminated with arsenic is a growing public health issue, which may increase the risk of cancer, peripheral vascular disease, liver, lung, and diabetes, as well as neurological abnormalities, affecting more than 100 million people in the world[1,2]. Nervous system diseases have always been the research focus, and the damage of nervous system caused by arsenic in the environment has also been widely concerned. Arsenic accumulated induce neurobehavioral function, like intelligence and memory of child and adult. For example, epidemiological studies by Wasserman GA arsenic exposure impairs child memory[3]. Furthermore, research on China adults and elders has indicated an association between excess arsenic intake from drinking water and cognitive impairment[4]. However, the mechanism of cognitive impairment induced by arsenic is still unclear.

Hippocampus is mainly responsible for learning, memory, cognition, spirit and other important functions related to behavior and intelligence. It is also one of the most vulnerable brain structures. Hippocampus is one of the main target organs of arsenic induced cognitive impairment. It is reported that arsenic induced rat hippocampal neurons abnormally apoptotic and damaged learning and

memory abilities[5]. Arsenic induces neurons damage through multiple mechanisms, including mitochondria-mediated apoptosis. Our previous studies have also shown that arsenic causes apoptosis of rat cerebellar granule neurons, which is related to arsenic breaking the balance between Bax and Bcl-2 (B-cell lymphoma-2)[6-8]. The Bcl-2 family members promote apoptosis through hydrolysis, dephosphorylation and other modifications. Apoptosis promoting members change their intracellular localization from cytoplasm to mitochondrial membrane, open mitochondrial permeability transport pore, reduce mitochondrial membrane potential, and apoptotic signal molecules such as Cytochrome C enter cytoplasm to activate caspase family cascade reaction [9-11]. ATP is consumed in the process of apoptosis, for example, ATP is necessary for chromatin condensation of apoptotic cells[12]. The maintenance and reduction of intracellular ATP levels are systematically regulated during apoptosis[13]. ATP synthase on the inner mitochondrial membrane uses the energy of mitochondrial membrane potential to synthesize ATP. When the mitochondrial permeability transport pore continues to open, the mitochondrial membrane potential decreases or even disintegrates completely, which reduces the content of ATP[14]. It is reported that arsenic exposure contributed to neuronal cells damage, accompanied ATP decrease [15-18]. The change of ATP is related to the synthesis of mitochondria.

One of the most important transcriptional coactivators affecting mitochondrial biogenesis is peroxisome proliferator activated receptor γ Coactivator α (PGC-1 α), PGC-1 α has selective activity to specific stimuli in different tissues, especially plays a major role in mitochondrial biogenesis and functional regulation, and participates in cell death and stress response. As previous studies have shown, the inhibition of PGC-1 α protein induces the disorder of mitochondrial dynamics and the apoptosis[19], activate PGC-1 α related signal pathway to play the role of anti-oxidation and anti-apoptosis[6]. As reported that in the process of apoptosis of HT22 induced by ischemia/reperfusion in vitro, the expression of PGC-1 α and Bcl-2 was decreased, and the expression of Bax was up-regulated, on the contrary, by increasing PGC-1 α and Bcl-2, down regulate the expression of Bax to reduce apoptosis[20]. In addition, the activation of PGC-1 α can improve the cognitive ability of aging related rats[21]. Therefore, it is necessary to explore the association of between PGC-1 α and ATP in arsenic-induced hippocampal nerve cell damage.

Hence, the present study aimed to explore the change of PGC-1 α in arsenic-induced rat hippocampus damage and analyze the relationship between arsenic, PGC-1 α , ATP and apoptosis in rat brain exposed (NaAsO₂, orally via drinking water) by different dose arsenic (0, 2, 10, and 50 mg/L).

2. Materials and methods

2.1. Materials and Reagents

Anti-PGC-1 α , Anti-Bcl-2, Anti-NeuN, and Anti-Bax were purchased from Abcam Ltd. (Abcam, Cambridge, UK). Cytochrome C was purchased from Cell Signaling Technology (Massachusetts, USA). TUNEL Assay Kit was purchased from *In Situ* Cell Death Detection Kit, POD (Roche Applied Science). ATP Content Assay Kit was purchased from Solarbio life science (Beijing Solarbio Science & Technology Co., Ltd.).

2.2. Animal and experimental designs

Male Wistar rats, 200-250g, were purchased from Charles River Laboratory Animal Technology Co., Ltd. The rats were reared in the laboratory environment with 12 hours of light dark cycle, 22 \pm 2°C and 50 \pm 5% RH of temperature and humidity respectively, and in the way of free drinking water and feeding. Forty rats were randomly divided into control group, low dose group, medium dose group and high dose group (n = 10). The rats in the four groups were exposed to 0, 2, 10, and 50 mg/L sodium arsenite (NaAsO₂, orally via drinking water) for 12 weeks. The protocol was approved by the requirements of the ethics committee of Harbin Medical University.

2.3. Hematoxylin-Eosin (H&E) Staining

The brains were fixed by 4% paraformaldehyde and embedded in paraffin. The brain samples were cut into 5 μm -thick sections. After that, the brain sections were dewaxed with xylene I and xylene II for 10 minutes each time. The dewaxed tissues were placed in 100% ethanol, 95% ethanol (I), 95% ethanol (II), 90% ethanol, 80% ethanol, 70% ethanol and distilled water for 5 minutes respectively, then soaked with hematoxylin for 10 minutes and differentiated with 1% hydrochloric acid ethanol for 1-3 seconds. After that, they were stained with eosin for 7 minutes. Then the slides were placed in 70% alcohol for 5 minutes, 80% alcohol for 5 minutes, 90% alcohol for 5 minutes, 95% alcohol for 5 minutes, 95% alcohol for 5 minutes, 100% alcohol (I) for 5 minutes, 100% alcohol (II) for 5 minutes, n-butanol (I) for 1 minute, n-butanol (II) for 1 minute for dehydration. Then the tissue slides were placed in xylene I and xylene II for transparency. Finally, the sections were sealed with neutral resin and observed under Olympus Bx53 microscope.

2.4. Terminal-deoxynucleotidyl Transferase Mediated Nick End Labeling (TUNEL) Assay

According to the manufacturer's instruction of In Situ Cell Death Detection Kit, we detected the apoptosis of CA1 region in hippocampus. The tissue sections were dewaxed and hydrated in xylene and different concentrations of ethanol. Then, the tissue was treated with 10 $\mu\text{g/mL}$ proteinase K on ice for 5 minutes. Subsequently, the slides were incubated with 50 μL of TUNEL reaction mixture at 37 $^{\circ}\text{C}$ for 60 minutes, followed by POD staining at 37 $^{\circ}\text{C}$ for 30 minutes. After DAB staining, the slides were stained by hematoxylin. Three slides were randomly selected from each group, and three fields (400 \times) were observed. TUNEL positive cells were observed under Olympus BX53 microscope. The positive cells in TUNEL assay were brown or brown yellow.

2.5. The ultrastructure of neurons in hippocampus was observed by transmission electron microscope (TEM)

The hippocampus was cut into about 1 mm^3 tissue block and fixed in 1.5 mL glutaraldehyde at 4 $^{\circ}\text{C}$. The fixed tissue was fixed with 1% osmic acid. Next, the tissues were placed in 30% acetone for 10 minutes, 50% acetone for 10 minutes, 70% acetone for 10 minutes, 90% acetone for 10 minutes, 100% acetone I for 10 minutes, 100% acetone II for 45 minutes, and 100% acetone III for 45 minutes. Then, it was placed in acetone and pure resin mixed solution for 1.5 hours, then embedded in pure resin and prepared slices. Finally, it was stained with uranyl acetate and lead citrate, and observed and photographed by transmission electron microscope.

2.6. Detection of Total Arsenic in Brain

Hydride generation atomic fluorescence spectrometry (HG-AFS) was used to detect the total arsenic content in rat brain tissue. The experimental method was in accordance with the Chinese national standard method (GB/T 5750.6-2006). Each sample was digested with a mixture of 900 μL concentrated nitric acid, 300 μL perchloric acid and 300 μL concentrated sulfuric acid to digest 0.1g brain tissue. Before detection, 1mL of thiourea ascorbic acid and 1 mL of concentrated hydrochloric acid were added to the digested sample respectively, and diluted to 10mL with deionized water. The standard solution was prepared with standard reference substance (GBW08611). Hydride generation atomic fluorescence spectrometer (AFS-933, Beijing Titan instruments, China) was used to detect the total arsenic level.

2.7. Immunohistochemistry

Immunohistochemical method was used to detect PGC-1 α , Bax, Cytochrome C, and Bcl-2. Brain paraffin slices were dewaxed and hydrated with xylene and ethanol, and then incubated with 0.3% hydrogen peroxide solution for 15 minutes. The slices were placed in citric acid buffer (pH6.0), and the antigen was repaired by microwave. 5% BSA was used to block at 37 $^{\circ}\text{C}$ for 30 minutes, then the slices were incubated with antibodies of PGC-1 α (1:500), Bax (1:200), Cytochrome C (1:150), and Bcl-2 (1:300) at 4 $^{\circ}\text{C}$ overnight. Next, the sections were incubated with Goat anti rabbit second antibody (BOSTER Biological Technology co.ltd, China) at 37 $^{\circ}\text{C}$ for 30 minutes. Then, the slices were incubated in DAB Staining Kit (BOSTER Biological Technology co. ltd, China), and stained with hematoxylin.

The positive cells were brown under light microscope. Each group was randomly selected three slices, each slice was selected three fields (400 ×). The average optical density of positive cells was observed, and the expression of PGC-1 α , Bax, Cytochrome C and Bcl-2 was analyzed by IPP software.

2.8. Immunofluorescence staining

Brain sections are dewaxed and hydrated. Next, the sections were incubated with PGC-1 α antibody (1:50) and NeuN (1:200) overnight at room temperature. After washing with PBS, the sections were incubated with Cy3 marked 570, FITC marked 520 secondary antibodies (1: 500) for two hours at room temperature followed by DAPI labeling and mounting in anti-fade medium. Images were collected with a Zeiss LSM-710 confocal microscope.

2.9. Detection of ATP contents in brain

According to the instructions of the kit, we detected the ATP content in brain tissue. Briefly, take about 0.1g tissue, add 1mL extraction solution, ice bath homogenization, 8000g 4°C centrifugation for 10 minutes, take the supernatant, then add 500uL chloroform, fully shake and mix, 10000g 4 °C centrifugation for 3 minutes, take the supernatant, and then process it as liquid. After full mixing, immediately measure the absorbance value A1 at 340nm for 10 seconds, and then put it into 37°C incubator for 3 minutes, and then measure the absorbance value A2. ATP content = $0.625 \times \Delta A$ determination/ ΔA standard/tissue quality.

2.10. Statistical Analysis

SPSS17.0 statistical software was used to analyze the experimental data. The mean optical density, arsenic contents in brain, and ATP contents in brain values were expressed as mean \pm SD. The Image-Pro Plus software was used to analyze mean optical density. One-way analysis of variance (ANOVA) was used to analyze data and followed by the least significant test (LSD test). The correlation between the mean optical density, ATP contents in brain, and arsenic in brain was based on Pearson correlation analysis. Difference was statistically significant at $P < 0.05$.

3. Results

3.1. Arsenic accumulated in brain and induced neuronal apoptosis

We previously reported the body weights of the rats from NaAsO₂ groups did not significantly change compared to control group in this study[22]. In order to understand the accumulation of arsenic in brain, arsenic content was detected by atomic fluorescence spectrometry. The arsenic contents of brain in 0, 2, 10 and 50 mg/L NaAsO₂ groups were 1.14 ± 0.98 , 1.47 ± 0.51 , 2.30 ± 0.75 , 3.03 ± 1.10 $\mu\text{g/g}$, respectively. These results showed that the arsenic level in brain increased in 2, 10, and 50 mg/L NaAsO₂ groups, compared with the control group ($P < 0.05$). With the increase of NaAsO₂ exposure dose, the brain arsenic content gradually increased. These results indicated that arsenic can accumulate in the brain (**Fig1A**).

We used H & E staining to observe the pathological changes of rat hippocampus. Under the microscope of 400 time, we clearly see the hippocampal formation composed of CA1, CA3 and dentate gyrus (DG). The CA3 area of hippocampus connects with the inferior dentate gyrus, extends inward into dentate gyrus, and extends outward into CA1 area. When magnified to 400 time, the cells in CA1 region of control group were well-organized, orderly and closely arranged, the cytoplasm was evenly red stained, the nucleus was large and round, dark blue, and the nucleolus was clear. Compared with the control group, the cells in each arsenic group showed different degrees of pathological changes, that is, with the increase of arsenic exposure, the cells in hippocampal CA1 area gradually decreased, arranged irregularly, and the shape was fuzzy, and some cells with unclear nuclear boundary and swelling. The results are shown in (**Fig1B**).

The hippocampal CA1 region nerve cells ultrastructure observed by transmission electron microscopy showed that the cells in the control group had clear outline, normal morphology, clear

and complete nuclear membrane, uniform chromatin, large number of mitochondria, long circle or oblate shape, orderly arrangement of internal ridge, complete structure. In the 2 mg/L NaAsO₂ group, increased lipofuscin and swollen mitochondria were observed in hippocampal nerve cells, which indicated that the nerve cells were under stress. In the 10 mg/L NaAsO₂ group, a slight disruption in the edge set of chromatin in the nucleus, swollen mitochondria, and reduced organelles were observed in nerve cells. In the 50 mg/L NaAsO₂ group, hippocampal nerve cells showed more severe alterations, such as, massive loss of organelles, disruption in the nuclear chromatin border set, loss of abnormal structural integrity of the nuclear membrane, and nerve cells showed apoptotic features (Fig1C).

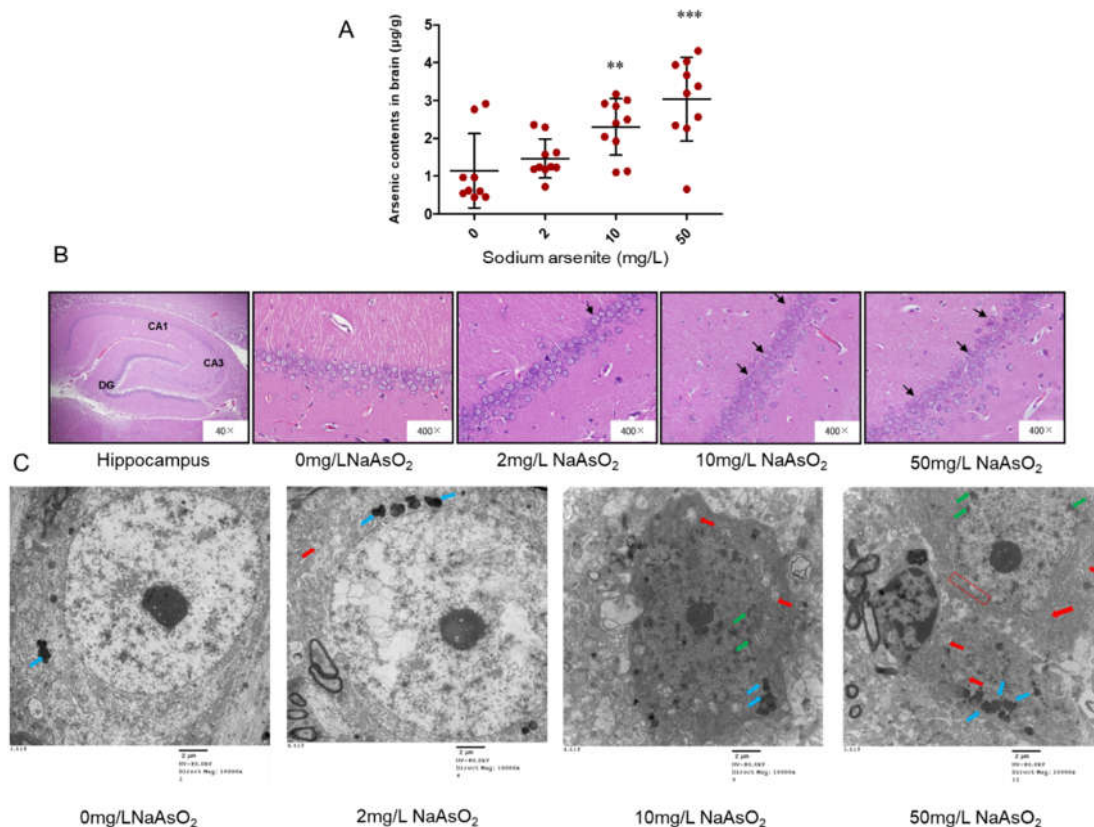


Figure 1. Arsenic contents, H&E staining and ultrastructural changes in the hippocampal CA1 region in the arsenic exposure rats. (A) Arsenic contents in brain of rats, n = 9-10. Results represent mean \pm SD (μ g/g). (B) H&E staining was observed in rat hippocampal CA1 region, n = 9-10. Abnormal cells were showed by black arrows. (C) The ultrastructure of neurons in the hippocampal CA1 region (scale bar = 2 μ m), n = 3. Blue arrows: accumulated lipofuscin. Red arrows: vacuolated mitochondrion. Green arrows: chromatin condensation and margination. Red box: the integrity of the nuclear membrane disappeared. **P < 0.01, ***P < 0.001 VS. control group.

3.2. TUNEL Analysis in the hippocampal CA1 of rats exposed to different arsenic concentrations

TUNEL staining was used to detect apoptosis in hippocampus of rats exposed to different doses of arsenic. Brown staining cells were TUNEL positive. The apoptosis rate was expressed as the percentage of TUNEL positive cells in the total number of cells. The results showed that the apoptotic cell ratio of hippocampus in control group, 2, 10 and 50 mg/L NaAsO₂ groups were 11.84 ± 2.27 , 20.40 ± 6.01 , 29.71 ± 2.18 , and 31.63 ± 1.06 , respectively. Compared with the control group, the apoptosis rate of 2, 10 and 50 mg/L NaAsO₂ groups increased significantly ($P < 0.05$), but there was no significant difference in the apoptosis rate between the 10 mg/L and 50 mg/L NaAsO₂ groups (Fig2A and Fig2B). The above results indicated that NaAsO₂ could induced nerve cells apoptosis, the apoptosis cells induced by high dose arsenic may reach a platform stage in this study.

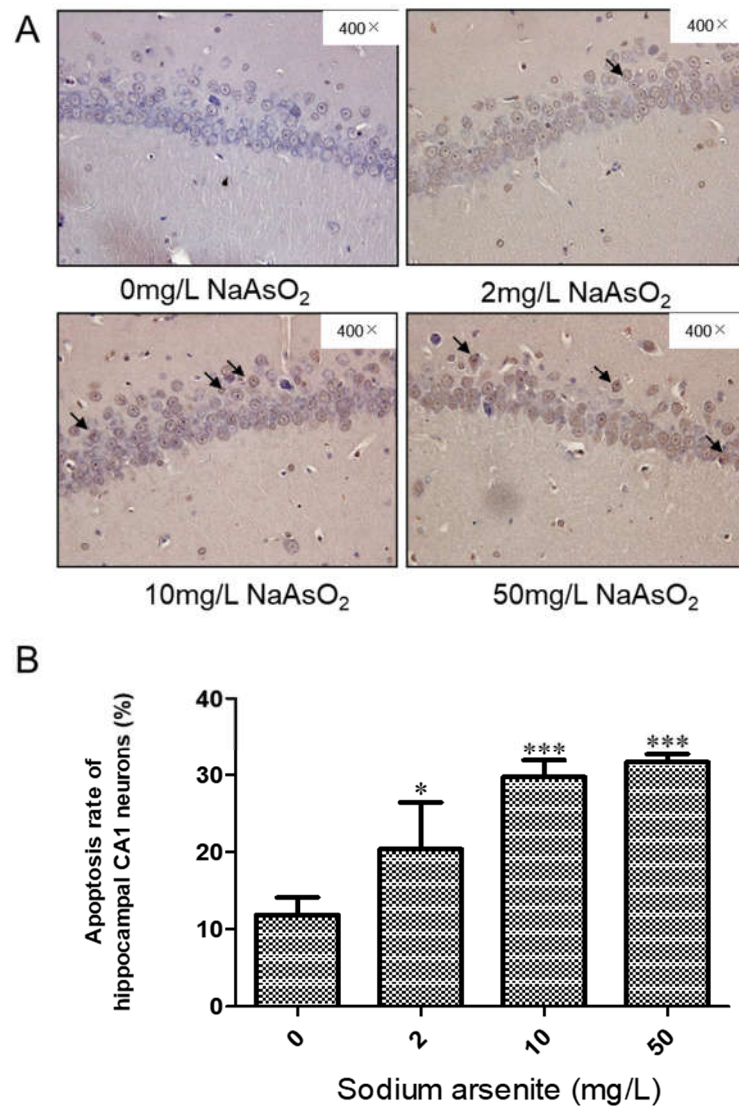


Figure 2. TUNEL analysis of the hippocampal CA1 region in the arsenic exposure groups. (A) Representative images of TUNEL-positive cells in the hippocampal CA1 region (magnification 400 \times). **(B)** Apoptotic ratio in the hippocampal CA1 region (Results represent mean \pm SD). * P < 0.05, *** P < 0.001 VS. control group, n = 3.

3.3. Bcl-2, Bax, and Cytochrome C expressions in hippocampal CA1 region of rats after arsenic exposure

Immunohistochemistry was used to analyze the effect of arsenic on Bcl-2, Bax, and Cytochrome C. Immunohistochemical results showed that the expression of Bcl-2, Bax, and Cytochrome C was positive in hippocampal CA1 area of rat brain, which showed that there were brown or brownish yellow granules in the cells. Compared with the control group, the level of Bcl-2 protein in 10 and 50 mg/L NaAsO₂ group decreased significantly (control group VS. 10 mg/L NaAsO₂ group, P < 0.01; control group VS. 50 mg/L NaAsO₂ group, P < 0.05; **Fig2A** and **Fig2D**). Compared with the control group, the level of Bax protein in 50 mg/L NaAsO₂ group increased significantly in dose-dependent manner (P < 0.001; **Fig2B** and **Fig2E**). Whereas the Bax/Bcl-2 ratio increased significantly in 50 mg/L NaAsO₂ group (P < 0.001; **Fig2F**). Furthermore, as shown in **Fig2C** and **Fig2G**, the expression level of Cytochrome C in the 2 and 50 mg/L NaAsO₂ group was significantly higher than that in control group (P < 0.05). These results indicated that NaAsO₂ induced mitochondrial pathway apoptosis.

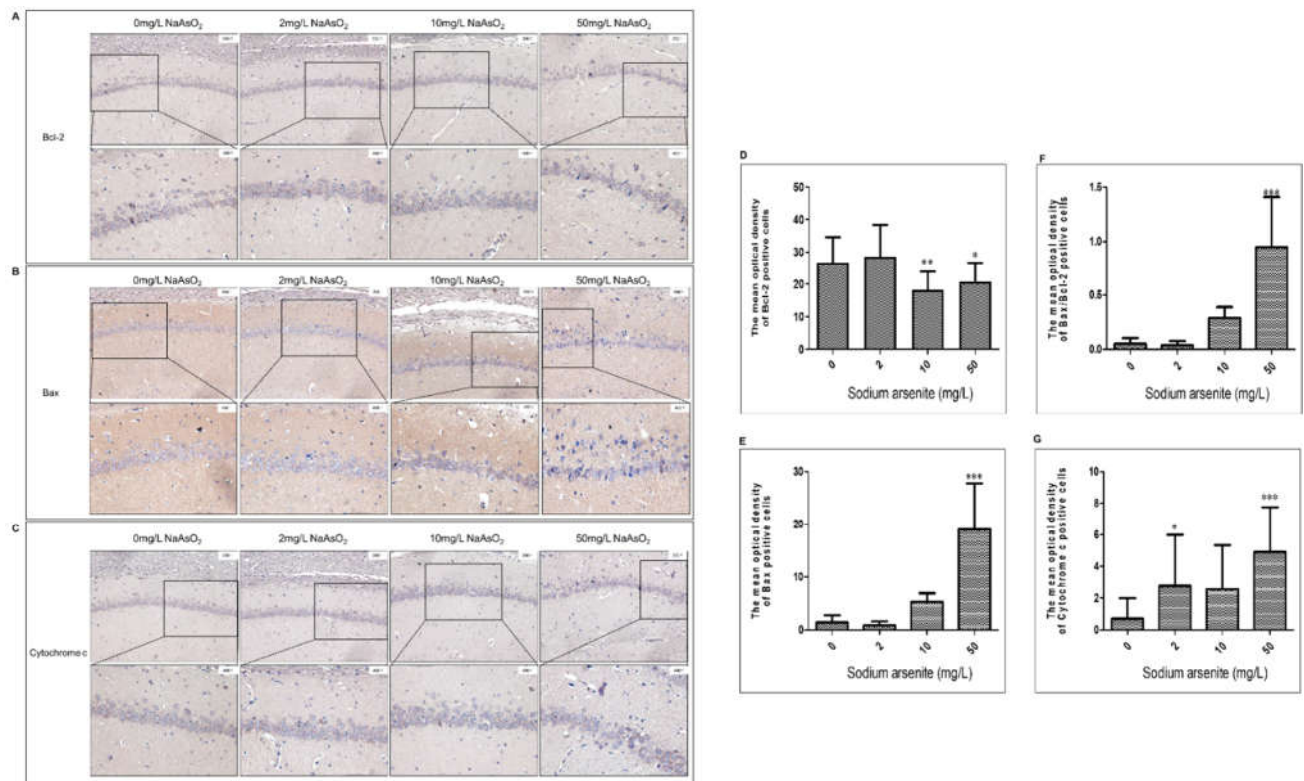


Figure 3. Bcl-2, Bax, and Cytochrome C expressions in hippocampus CA1 region of rats after arsenic exposure. (A), (B) and (C) Representative images of Bcl-2, Bax and Cytochrome C in the hippocampal CA1 region (magnification 200×, 400×), respectively. **(D), (E), (F) and (G)** Representative the mean optical density analysis of the Bcl-2, Bax, the ratio of Bax/Bcl-2 and Cytochrome C (Results represent mean ± SD). * $P < 0.05$, ** $P < 0.01$, *** $P < 0.001$ VS. control group.

3.4. PGC-1 α expression in hippocampal CA1 region of rats exposed to different arsenic concentrations

Immunohistochemistry and immunofluorescence were used to observe the effect of arsenic on PGC-1 α that is a major regulator of mitochondrial biogenesis and function in hippocampal CA1 region of rats. Immunohistochemistry showed that PGC-1 α expression in hippocampal CA1 neurons decreased after arsenic exposure. (**Fig4A** and **Fig4C**). In order to further analyze the relationship between PGC-1 and arsenic in rat brain, we analyzed the correlation between PGC-1 α and brain arsenic. The results showed that the expression of PGC-1 α was negatively correlated with arsenic in rat brain, and the correlation coefficient was $r = -0.526$ ($P < 0.05$, **Fig4B**), that is, with the increase of arsenic in rat brain, the PGC-1 α expression gradually decreased. The results of immunofluorescence showed that PGC-1 α positive cells expressed red granules in cytoplasm and nucleus, the positive cells of PGC-1 α decreased in hippocampal CA1 area in the arsenic exposure rats (**Fig4C**). These results showed that PGC-1 α decrease was related to arsenic.

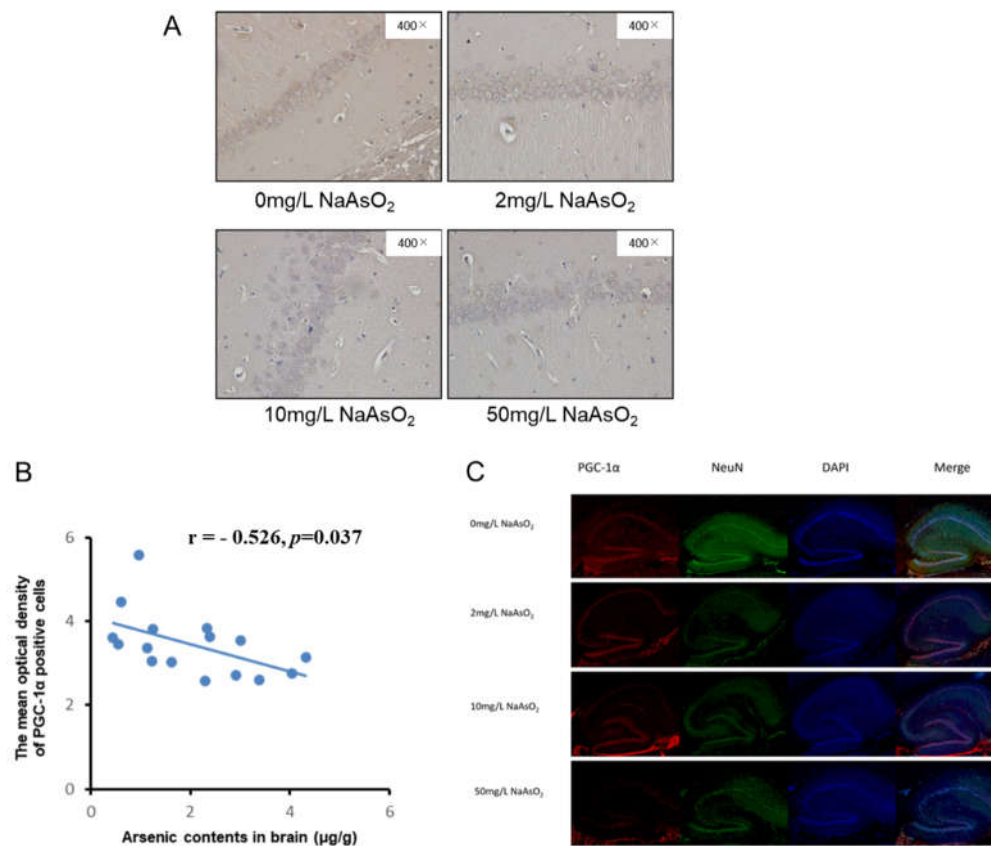


Figure 4. The changes of PGC-1 α expression in the hippocampus after arsenic exposure. **(A)** and **(C)** Representative immunohistochemical (magnification 400 \times) and immunofluorescence (magnification 20 \times) images of PGC-1 α in the hippocampal CA1 region, respectively. PGC-1 α labeled in red, NeuN labeled in green, DAPI labeled in blue. **(B)** Representative image of correlation analysis between PGC-1 α expression (the mean optical density of immunohistochemical) in hippocampal CA1 region and brain arsenic, $n = 4$.

3.5. Correlation analysis between brain ATP, arsenic and PGC-1 α expression

PGC-1 α is a potent regulator of mitochondrial biogenesis and energy metabolism and affects the generation of ATP. Therefore, we detected the changes of brain ATP content in each group and analyzed the correlation between ATP, PGC-1 α , brain arsenic content and apoptosis. As shown in the figure **Fig5A**, brain arsenic content showed a negative correlation with brain ATP, and the correlation coefficient $r = -0.332$ ($P < 0.05$), indicating that ATP content gradually decreased with the increase of brain arsenic content. As shown in the figure **Fig5B and 5C**, the correlation coefficient between ATP contents and PGC-1 α expression (immunohistochemical mean optical density) was $r = 0.610$, and the correlation coefficient between PGC-1 α expression (average optical density of immunohistochemical) and apoptosis was $r = -0.598$, but there was no significant correlation relationship between ATP contents and apoptosis (**Fig5D**).

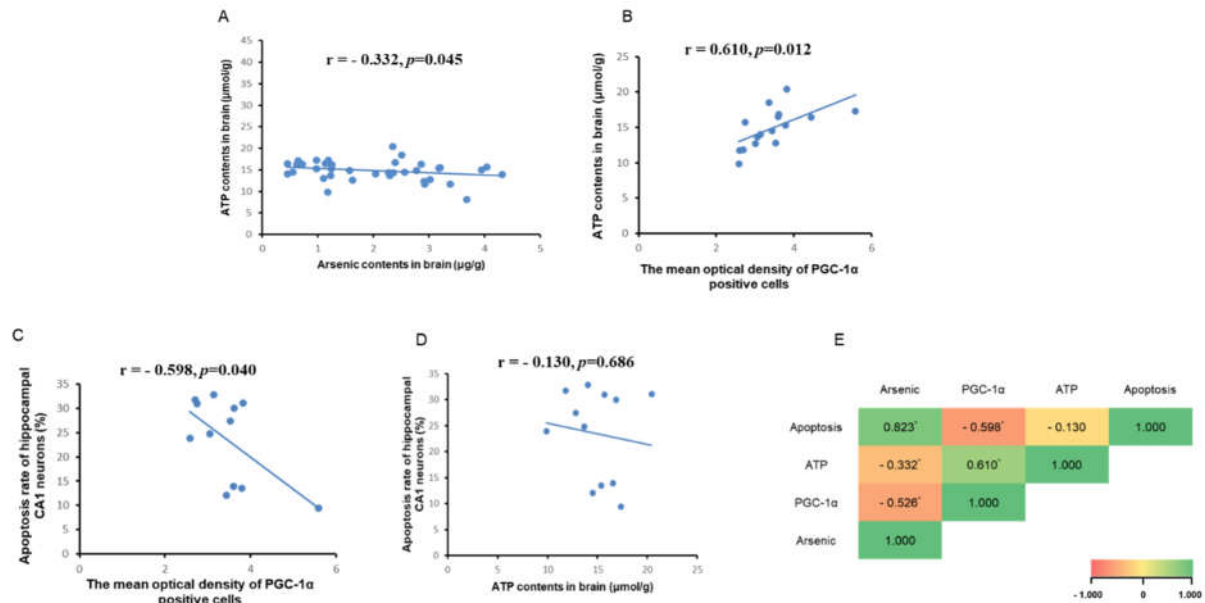


Figure 5. Correlation analysis between brain ATP, arsenic and PGC-1α expression. (A) Correlation analysis between ATP contents and arsenic contents in brain. (B) Correlation analysis between ATP contents and PGC-1α immunohistochemical mean optical density. (C) Correlation analysis between apoptosis and PGC-1α immunohistochemical mean optical density. (D) Correlation analysis between apoptosis and ATP contents. (E) Correlation analysis between arsenic, PGC-1α, ATP, and apoptosis in brain. * $P < 0.05$.

4. Discussion

In this study, a rat model of arsenic exposure was established by orally via drinking water. Our previous study reported that the arsenic levels in the serum and urine were both significantly increased in the arsenic exposure groups compared to the controls, and had no effect on body weights in this study[22]. In this study, we detected brain arsenic contents in arsenic exposure rats. These results showed that with the increase of arsenic exposure, the contents of arsenic in brain increased, indicating that arsenic can be accumulated in brain by drinking water. Then, the pathological changes of neurons in hippocampal CA1 area in each group were observed. In the control group, the neurons in CA1 area were layered, arranged neatly and closely, with clear nucleoli and uniform cytoplasm. With the increase of arsenic exposure dose, arranged in disorder, blurred cell outline, and some unclear nuclear boundary and swollen cells were seen in CA1 area. The ultrastructural results also showed that with the change of NaAsO₂ concentration, the number of mitochondria in hippocampal nerve cells decreased in varying degrees and the structure was incomplete. Meanwhile, with the increase of NaAsO₂ concentration, the level of apoptosis rate increased significantly, but no markedly increased apoptosis between 10mg/L NaAsO₂ group and 50mg/L NaAsO₂ group, this speculated that apoptotic cells in hippocampal CA1 region reached saturation in the 50mg/L NaAsO₂ group in this study. The above indicated that the rat model of arsenic exposure is successfully constructed, and suggests that arsenic cause neuronal apoptosis in hippocampus CA1, accompanied by mitochondrial and other ultrastructural damage, which is consistent with the results of other studies[5,23].

Apoptosis is induced by endogenous and exogenous apoptotic pathways, while mitochondrial apoptosis pathway is the executor of endogenous apoptosis process. It is reported that arsenic through changing apoptosis-related proteins Bax and Bcl-2 expression damage rat hippocampus[24]. The regulation of apoptosis in mitochondrial pathway involves many mechanisms, including the opening of MPTP[25], the release of apoptosis and anti-apoptotic proteins, causing or inhibiting caspase cascade reaction and destroying mitochondrial membrane structure[26]. As previous studies have showed that the release of apoptosis promoting proteins such as apoptosis initiation factor Cytochrome C, apoptosis promoter and apoptosis effector caspase family, SMAC family and Bax

induce apoptosis[27], Bcl-2 and IAPs family can inhibit apoptosis by inhibiting the release of apoptotic proteins[28]. Apoptosis related cascades are interrelated and produce apoptosis effect. Among many apoptotic and anti-apoptotic gene families, Bcl-2 family plays an important role in regulating mitochondrial membrane permeability, cascade reaction of caspase family proteins and changes of membrane potential. Among them, Bax can increase mitochondrial membrane permeability, form macromolecular channels, and make some macromolecules enter the cytoplasm, leading to swelling of mitochondria and initiating the mechanism of apoptosis, in addition, it also acts with transcription factor p53 to affect the membrane permeability of mitochondria, resulting in the loss of membrane potential[7,29]. Bcl-2 inhibit the production of excess reactive oxygen species, increase the load of calcium, block the cascade of caspase and inhibit apoptosis[30]. In this study, Bax, Bcl-2 and Cytochrome C expression in hippocampal CA1 region of rats in each group was detected. The results showed that arsenic increased Bax, Cytochrome C expression and decreased Bcl-2 expression. The above, which is consistent with other studies, shows that arsenic induces neuronal apoptosis in rat hippocampal CA1 region at least through the mitochondrial pathway[31].

Mitochondria produce adenosine triphosphate through oxidative phosphorylation of the electron transport chain, which produces byproducts such as ROS accumulation to induce oxidative stress [32], and the expression increase of Cytochrome C leads to apoptosis[33,34]. On the other hand, mitochondria can also counteract the damage caused by oxidative stress and apoptosis[32]. Previous study has shown that arsenic induced nerve cell damage is also associated with PGC1- α , which is closely related to mitochondrial biogenesis[35]. PGC-1 α is a main regulator of mitochondrial biogenesis including mitochondrial quality regulation mechanisms such as division, fusion and mitosis and also affects mitochondrial function such as energy metabolism anti-oxidative stress, and anti-apoptosis[36-41]. Some studies have shown that oxidative damage, mitochondrial biogenesis imbalance, and a decrease in PGC-1 α and ATP are important injury characteristics of neurodegenerative diseases[42,43]. When agonists are used to promote PGC-1 α expression, ATP increases, mitochondrial dependent cell apoptosis pathway proapoptotic protein Bax downregulates, and anti-apoptotic protein Bcl-2 upregulates, alleviating neuronal damage[44]. It is also reported that overexpressed PGC-1 α decreased apoptosis[41,43]. In this study, PGC-1 α level of hippocampus was decreased in arsenic exposed rat. In order to further analyze the association between PGC-1 α and brain arsenic, we analyzed the correlation between PGC-1 α and arsenic, the result showed that arsenic has negative effect on PGC-1 α expression in brain in arsenic exposure rat. Then, we analyzed effect of arsenic on mitochondrial apoptosis pathway and PGC-1 α expression in this study, the result showed that there was a negative correlation between apoptosis and PGC-1 α , which suggested that PGC-1 α plays an important role in arsenic induced hippocampal neuronal cells apoptosis. Previous studies have shown that brain ATP content is regulated by PGC-1 α , and the decrease of PGC-1 α reduces the content of ATP[45-47]. In this study, there was positive correlation between PGC-1 α and ATP contents. In addition, there was a negative correlation between arsenic in rat brain and ATP content in brain tissue, that is, arsenic in brain decreased ATP content, but the results did not show an obvious relationship between the reduction of ATP and apoptosis, which may be due to the involvement of other mechanisms in the process of arsenic affecting energy metabolism. Some limitations of this study should be noted. The detailed mechanism needs we further exploration in the future.

5. Conclusion

The present study found that arsenic induced rat hippocampal neuronal cells mitochondrial pathway apoptosis, accompanied by incomplete mitochondrial structure, PGC-1 α expression decrease, and ATP reduction. In addition, we also found that brain arsenic has negative effects on PGC-1 α and ATP, PGC-1 α expression and ATP contents in brain was negatively with the contents of brain arsenic, PGC-1 α expression was negatively with apoptosis hippocampal CA1 region, PGC-1 α expression was positively with ATP contents in brain, but no obvious linear relationship between the ATP and apoptosis, which may mean ATP reduction is not the direct result of arsenic induced nerve

cell apoptosis. This study contributes to provides novel insight into broader mechanisms by which arsenic injury hippocampus.

CRedit authorship contribution statement: Bo Ding & Xinbo Ma & Yang Liu: Methodology, Writing - review & editing. Bangyao Ni & Siqi Lu & Yuting Chen: Methodology. Xiaona Liu: Roles - original draft, Data curation, Software, Founding acquisition. Wei Zhang: Conceptualization, Roles- review & editing, Founding acquisition.

Declaration of competing interest: The authors have no conflicts of interest about this article.

Acknowledgments: The study was financially supported by National Natural Science Foundation of China (Grant No. 81,803,176 and 81402636), HMU Marshal Initiative Funding (Grant No. HMUMIF-21014), and Heilongjiang Provincial Postdoctoral Science Foundation (Grant NO. LBH-Z18170).

References

- Hong, Y.S.; Song, K.H.; Chung, J.Y. Health effects of chronic arsenic exposure. *J Prev Med Public Health* **2014**, *47*, 245-252, doi:10.3961/jpmph.14.035.
- Raju, N.J. Arsenic in the geo-environment: A review of sources, geochemical processes, toxicity and removal technologies. *Environ Res* **2022**, *203*, 111782, doi:10.1016/j.envres.2021.111782.
- Wasserman, G.A.; Liu, X.; Parvez, F.; Ahsan, H.; Factor-Litvak, P.; Geen, A.V.; Slavkovich, V.; Lolacono, N.J.; Cheng, Z.; Hussain, I. Water Arsenic Exposure and Children's Intellectual Function in Araihaazar, Bangladesh. *Environmental Health Perspectives* **2004**, *112*, 1329-1333.
- Liu, J.; Gao, Y.; Liu, H.; Sun, J.; Liu, Y.; Wu, J.; Li, D.; Sun, D. Assessment of relationship on excess arsenic intake from drinking water and cognitive impairment in adults and elders in arsenicosis areas. *Int J Hyg Environ Health* **2017**, *220*, 424-430, doi:10.1016/j.ijheh.2016.12.004.
- Sun, H.; Yang, Y.; Shao, H.; Sun, W.; Gu, M.; Wang, H.; Jiang, L.; Qu, L.; Sun, D.; Gao, Y. Sodium Arsenite-Induced Learning and Memory Impairment Is Associated with Endoplasmic Reticulum Stress-Mediated Apoptosis in Rat Hippocampus. *Frontiers in molecular neuroscience* **2017**, *10*, 286, doi:10.3389/fnmol.2017.00286.
- Wang, P.; Zhao, M.; Chen, Z.; Wu, G.; Fujino, M.; Zhang, C.; Zhou, W.; Zhao, M.; Hirano, S.I.; Li, X.K.; et al. Hydrogen Gas Attenuates Hypoxic-Ischemic Brain Injury via Regulation of the MAPK/HO-1/PGC-1 α Pathway in Neonatal Rats. *Oxid Med Cell Longev* **2020**, *2020*, 6978784, doi:10.1155/2020/6978784.
- Wang, Y.; Bai, C.; Guan, H.; Chen, R.; Wang, X.; Wang, B.; Jin, H.; Piao, F. Subchronic exposure to arsenic induces apoptosis in the hippocampus of the mouse brains through the Bcl-2/Bax pathway. *J Occup Health* **2015**, *57*, 212-221, doi:10.1539/joh.14-0226-OA.
- Chen, F.; Zhou, C.C.; Yang, Y.; Liu, J.W.; Yan, C.H. GM1 Ameliorates Lead-Induced Cognitive Deficits and Brain Damage Through Activating the SIRT1/CREB/BDNF Pathway in the Developing Male Rat Hippocampus. *Biological trace element research* **2019**, *190*, 425-436, doi:10.1007/s12011-018-1569-6.
- Wang, Y.; Wang, S.; Cui, W.; He, J.; Wang, Z.; Yang, X. Olive leaf extract inhibits lead poisoning-induced brain injury. *Neural regeneration research* **2013**, *8*, 2021-2029, doi:10.3969/j.issn.1673-5374.2013.22.001.
- Lan, W.; Lin, J.; Liu, W.; Wang, F.; Xie, Y. Sulfiredoxin-1 protects spinal cord neurons against oxidative stress in the oxygen-glucose deprivation/reoxygenation model through the bax/cytochrome c/caspase 3 apoptosis pathway. *Neuroscience letters* **2021**, *744*, 135615, doi:10.1016/j.neulet.2020.135615.
- Zhu, X.; Yao, Y.; Guo, M.; Li, J.; Yang, P.; Xu, H.; Lin, D. Sevoflurane increases intracellular calcium to induce mitochondrial injury and neuroapoptosis. *Toxicology letters* **2021**, *336*, 11-20, doi:10.1016/j.toxlet.2020.11.002.
- Kass, G.E.; Eriksson, J.E.; Weis, M.; Orrenius, S.; Chow, S.C. Chromatin condensation during apoptosis requires ATP. *The Biochemical journal* **1996**, *318* (Pt 3), 749-752, doi:10.1042/bj3180749.
- Imamura, H.; Sakamoto, S.; Yoshida, T.; Matsui, Y.; Penuela, S.; Laird, D.W.; Mizukami, S.; Kikuchi, K.; Kakizuka, A. Single-cell dynamics of pannexin-1-facilitated programmed ATP loss during apoptosis. *eLife* **2020**, *9*, doi:10.7554/eLife.61960.
- Luis-García, E.R.; Becerril, C.; Salgado-Aguayo, A.; Aparicio-Trejo, O.E.; Romero, Y.; Flores-Soto, E.; Mendoza-Milla, C.; Montaña, M.; Chagoya, V.; Pedraza-Chaverri, J.; et al. Mitochondrial Dysfunction and Alterations in Mitochondrial Permeability Transition Pore (mPTP) Contribute to Apoptosis Resistance in Idiopathic Pulmonary Fibrosis Fibroblasts. *International journal of molecular sciences* **2021**, *22*, doi:10.3390/ijms22157870.
- Nino, S.A.; Morales-Martinez, A.; Chi-Ahumada, E.; Carrizales, L.; Salgado-Delgado, R.; Perez-Severiano, F.; Diaz-Cintra, S.; Jimenez-Capdeville, M.E.; Zarazua, S. Arsenic Exposure Contributes to the Bioenergetic Damage in an Alzheimer's Disease Model. *ACS Chem Neurosci* **2019**, *10*, 323-336, doi:10.1021/acschemneuro.8b00278.

16. Dua, T.K.; Dewanjee, S.; Gangopadhyay, M.; Khanra, R.; Zia-Ul-Haq, M.; De Feo, V. Ameliorative effect of water spinach, *Ipomea aquatica* (Convolvulaceae), against experimentally induced arsenic toxicity. *J Transl Med* **2015**, *13*, 81, doi:10.1186/s12967-015-0430-3.
17. Baldissarelli, L.A.; Capiotti, K.M.; Bogó, M.R.; Ghisleni, G.; Bonan, C.D. Arsenic alters behavioral parameters and brain ectonucleotidases activities in zebrafish (*Danio rerio*). *Comp Biochem Physiol C Toxicol Pharmacol* **2012**, *155*, 566-572, doi:10.1016/j.cbpc.2012.01.006.
18. Dwivedi, N.; Mehta, A.; Yadav, A.; Binukumar, B.K.; Gill, K.D.; Flora, S.J. MiADMSA reverses impaired mitochondrial energy metabolism and neuronal apoptotic cell death after arsenic exposure in rats. *Toxicol Appl Pharmacol* **2011**, *256*, 241-248, doi:10.1016/j.taap.2011.04.004.
19. Zheng, X.; Li, S.; Li, J.; Lv, Y.; Wang, X.; Wu, P.; Yang, Q.; Tang, Y.; Liu, Y.; Zhang, Z. Hexavalent chromium induces renal apoptosis and autophagy via disordering the balance of mitochondrial dynamics in rats. *Ecotoxicol Environ Saf* **2020**, *204*, 111061, doi:10.1016/j.ecoenv.2020.111061.
20. Yan, X.; Yu, A.; Zheng, H.; Wang, S.; He, Y.; Wang, L. Calycosin-7-O- β -D-glucoside Attenuates OGD/R-Induced Damage by Preventing Oxidative Stress and Neuronal Apoptosis via the SIRT1/FOXO1/PGC-1 α Pathway in HT22 Cells. *Neural Plast* **2019**, *2019*, 8798069, doi:10.1155/2019/8798069.
21. Yu, Y.; Zhao, Y.; Teng, F.; Li, J.; Guan, Y.; Xu, J.; Lv, X.; Guan, F.; Zhang, M.; Chen, L. Berberine Improves Cognitive Deficiency and Muscular Dysfunction via Activation of the AMPK/SIRT1/PGC-1 α Pathway in Skeletal Muscle from Naturally Aging Rats. *J Nutr Health Aging* **2018**, *22*, 710-717, doi:10.1007/s12603-018-1015-7.
22. Guo, X.; Fu, X.; Liu, X.; Wang, J.; Li, Z.; Gao, L.; Li, Y.; Zhang, W. Role of Pigment Epithelium-Derived Factor in Arsenic-Induced Vascular Endothelial Dysfunction in a Rat Model. *Biological trace element research* **2019**, *190*, 405-413, doi:10.1007/s12011-018-1559-8.
23. Bai, L.; Tang, Q.; Zou, Z.; Meng, P.; Tu, B.; Xia, Y.; Cheng, S.; Zhang, L.; Yang, K.; Mu, S.; et al. m6A Demethylase FTO Regulates Dopaminergic Neurotransmission Deficits Caused by Arsenite. *Toxicol Sci* **2018**, *165*, 431-446, doi:10.1093/toxsci/kfy172.
24. Mehta, K.; Kaur, B.; Pandey, K.K.; Dhar, P.; Kaler, S. Resveratrol protects against inorganic arsenic-induced oxidative damage and cytoarchitectural alterations in female mouse hippocampus. *Acta Histochem* **2021**, *123*, 151792, doi:10.1016/j.acthis.2021.151792.
25. Li, Y.; Sun, J.; Wu, R.; Bai, J.; Hou, Y.; Zeng, Y.; Zhang, Y.; Wang, X.; Wang, Z.; Meng, X. Mitochondrial MPTP: A Novel Target of Ethnomedicine for Stroke Treatment by Apoptosis Inhibition. *Front Pharmacol* **2020**, *11*, 352, doi:10.3389/fphar.2020.00352.
26. Brenner, C.; Kroemer, G. Apoptosis. Mitochondria--the death signal integrators. *Science* **2000**, *289*, 1150-1151, doi:10.1126/science.289.5482.1150.
27. Altnauer, F.; Conus, S.; Cavalli, A.; Folkers, G.; Simon, H.U. Calpain-1 regulates Bax and subsequent Smac-dependent caspase-3 activation in neutrophil apoptosis. *J Biol Chem* **2004**, *279*, 5947-5957, doi:10.1074/jbc.M308576200.
28. Binju, M.; Amaya-Padilla, M.A.; Wan, G.; Gunosewoyo, H.; Suryo Rahmanto, Y.; Yu, Y. Therapeutic Inducers of Apoptosis in Ovarian Cancer. *Cancers (Basel)* **2019**, *11*, doi:10.3390/cancers11111786.
29. Cregan, S.P.; MacLaurin, J.G.; Craig, C.G.; Robertson, G.S.; Nicholson, D.W.; Park, D.S.; Slack, R.S. Bax-dependent caspase-3 activation is a key determinant in p53-induced apoptosis in neurons. *The Journal of neuroscience : the official journal of the Society for Neuroscience* **1999**, *19*, 7860-7869, doi:10.1523/jneurosci.19-18-07860.1999.
30. Won, S.J.; Kim, D.Y.; Gwag, B.J. Cellular and molecular pathways of ischemic neuronal death. *J Biochem Mol Biol* **2002**, *35*, 67-86, doi:10.5483/bmbrep.2002.35.1.067.
31. Zhang, W.; Feng, H.; Gao, Y.; Sun, L.; Wang, J.; Li, Y.; Wang, C.; Zhao, L.; Hu, X.; Sun, H.; et al. Role of pigment epithelium-derived factor (PEDF) in arsenic-induced cell apoptosis of liver and brain in a rat model. *Biol Trace Elem Res* **2013**, *151*, 269-276, doi:10.1007/s12011-012-9558-7.
32. Chen, S.D.; Yang, D.I.; Lin, T.K.; Shaw, F.Z.; Liou, C.W.; Chuang, Y.C. Roles of Oxidative Stress, Apoptosis, PGC-1 α and Mitochondrial Biogenesis in Cerebral Ischemia. *International Journal of Molecular Sciences* **2011**.
33. Du, J.; Hang, P.; Pan, Y.; Feng, B.; Zheng, Y.; Chen, T.; Zhao, L.; Du, Z. Inhibition of miR-23a attenuates doxorubicin-induced mitochondria-dependent cardiomyocyte apoptosis by targeting the PGC-1 α /Drp1 pathway. *Toxicology and applied pharmacology* **2019**, *369*, 73-81, doi:10.1016/j.taap.2019.02.016.
34. Jia, N.; Sun, Q.; Su, Q.; Dang, S.; Chen, G. Taurine promotes cognitive function in prenatally stressed juvenile rats via activating the Akt-CREB-PGC1 α pathway. *Redox biology* **2016**, *10*, 179-190, doi:10.1016/j.redox.2016.10.004.
35. Prakash, C.; Kumar, V. Arsenic-induced mitochondrial oxidative damage is mediated by decreased PGC-1 α expression and its downstream targets in rat brain. *Chemico-Biological Interactions* **2016**, 228-235.
36. Halling, J.F.; Pilegaard, H. PGC-1 α -mediated regulation of mitochondrial function and physiological implications. *Applied physiology, nutrition, and metabolism = Physiologie appliquee, nutrition et metabolisme* **2020**, *45*, 927-936, doi:10.1139/apnm-2020-0005.

37. Navazani, P.; Vaseghi, S.; Hashemi, M.; Shafaati, M.R.; Nasehi, M. Effects of Treadmill Exercise on the Expression Level of BAX, BAD, BCL-2, BCL-XL, TFAM, and PGC-1 α in the Hippocampus of Thimerosal-Treated Rats. *Neurotoxicity research* **2021**, *39*, 1274-1284, doi:10.1007/s12640-021-00370-w.
38. Tritos, N.A.; Mastaitis, J.W.; Kokkotou, E.G.; Puigserver, P.; Spiegelman, B.M.; Maratos-Flier, E. Characterization of the peroxisome proliferator activated receptor coactivator 1 alpha (PGC 1alpha) expression in the murine brain. *Brain research* **2003**, *961*, 255-260, doi:10.1016/s0006-8993(02)03961-6.
39. Chen, S.D.; Yang, D.I.; Lin, T.K.; Shaw, F.Z.; Liou, C.W.; Chuang, Y.C. Roles of oxidative stress, apoptosis, PGC-1 α and mitochondrial biogenesis in cerebral ischemia. *International journal of molecular sciences* **2011**, *12*, 7199-7215, doi:10.3390/ijms12107199.
40. Szalardy, L.; Zadori, D.; Plangar, I.; Vecsei, L.; Weydt, P.; Ludolph, A.C.; Klivenyi, P.; Kovacs, G.G. Neuropathology of partial PGC-1 α deficiency recapitulates features of mitochondrial encephalopathies but not of neurodegenerative diseases. *Neuro-degenerative diseases* **2013**, *12*, 177-188, doi:10.1159/000346267.
41. St-Pierre, J.; Drori, S.; Uldry, M.; Silvaggi, J.M.; Rhee, J.; Jager, S.; Handschin, C.; Zheng, K.; Lin, J.; Yang, W.; et al. Suppression of reactive oxygen species and neurodegeneration by the PGC-1 transcriptional coactivators. *Cell* **2006**, *127*, 397-408, doi:10.1016/j.cell.2006.09.024.
42. Zhang, Q.; Lei, Y.H.; Zhou, J.P.; Hou, Y.Y.; Meng, H. Role of PGC-1 α in Mitochondrial Quality Control in Neurodegenerative Diseases. *Neurochemical Research* **2019**, *44*.
43. Chen, Z.; Tao, S.; Li, X.; Yao, Q. Resistin destroys mitochondrial biogenesis by inhibiting the PGC-1 α /NRF1/TFAM signaling pathway. *Biochemical and Biophysical Research Communications* **2018**, *504*, S0006291 \times 18317017-.
44. Mostafa Tork, O.; Ahmed Rashed, L.; Bakr Sadek, N.; Abdel-Tawab, M.S. Targeting Altered Mitochondrial Biogenesis in the Brain of Diabetic Rats: Potential Effect of Pioglitazone and Exendin-4. *Rep Biochem Mol Biol* **2019**, *8*, 287-300.
45. Nasehi, M.; Torabinejad, S.; Hashemi, M.; Vaseghi, S.; Zarrindast, M.R. Effect of cholestasis and NeuroAid treatment on the expression of Bax, Bcl-2, Pgc-1 α and Tfam genes involved in apoptosis and mitochondrial biogenesis in the striatum of male rats. *Metabolic brain disease* **2020**, *35*, 183-192, doi:10.1007/s11011-019-00508-y.
46. Xuefei; Zhang; Xiaoqing; Ren; Qi; Zhang; Zheyi; Li; Shuaipeng; Ma. PGC-1 α /ERR α -Sirt3 Pathway Regulates DAergic Neuronal Death by Directly Deacetylating SOD2 and ATP Synthase β . *Antioxidants & Redox Signaling* **2016**.
47. Yang, L.; Jiang, Y.; Xiaoqian, Y.E.; You, Y.; Lin, L.; Lian, J.; Juan, L.I.; Yang, S.; Xue, X. The neuroprotection of electro-acupuncture via the PGC-1 α /TFAM pathway in transient focal cerebral ischemia rats. *BIOCELL* **2022**, *046*.